Supplementary Information for:

Dimensional distribution and localization of amphiboles retrieved from human alveolar epithelial cells

*Ruggero Vigliaturo[a,b], Maja Jamnik[c], Goran Dražić[d], Marjetka Podobnik[c], Magda Tušek Žnidarič[e], Giancarlo Della Ventura[f,g,h], Günther J. Redhammer[i], Nada Žnidaršič[j], Simon Caserman[c], Reto Gieré[k,l]

[a]Department of Earth Sciences, University of Torino, Torino, Italy

[b]Interdepartmental Centre for Studies on Asbestos and Other Toxic Particulates, University of Torino, Torino, Italy

[c]Department of Molecular Biology and Nanobiotechnology, National Institute of Chemistry, Ljubljana, Slovenia

[d]Department of Materials Chemistry, National Institute of Chemistry, Ljubljana, Slovenia

[e]Department of Biotechnology and System Biology, National Institute of Biology, Ljubljana, Slovenia

[f]Department of Geological Sciences, University of Roma Tre, Roma, Italy

[g]INFN-Istituto Nazionale di Fisica Nucleare, Frascati (Rome), Italy

[h]INGV, Via di Vigna Murata 605, 00143 Roma, Italy

[i]Department of Materials Science & Physics, University of Salzburg, 5020 Salzburg, Austria

[j]Department of Biology, Biotechnical Faculty, University of Ljubljana, Ljubljana, Slovenia

[k]Department of Earth and Environmental Science, University of Pennsylvania, Philadelphia, U.S.A.

[l]Center of Excellence in Environmental Toxicology, University of Pennsylvania, U.S.A.

*Corresponding author: Ruggero Vigliaturo, ruggero.vigliaturo@unito.it

Recalculated dimensional parameters and aspect ratio of the amphibole particles before the interaction with the AECs

To compare the actual differences in the size distribution between the starting material and the material after the interaction, we restricted the dimensional range of interest to that determined for the minerals retrieved from the cells after exposure. The recalculated dimensional distribution for the starting material, as shown in Fig. S1, thus reflects the range determined by the maximum and minimum dimensions of the *retrieved* particles (i.e., particles after the interaction).

The dimensional distributions of the particles before and after the interaction with the AECs within the same dimensional range (determined by the maximum and minimum dimensions of the particles present in the cells) are similar in terms of w and L/w, whereas the width has a higher "dispersion" in terms of σ_{n-1} (noise). With respect to the particle population of the starting material within the range determined by the maximum and minimum dimensions of the retrieved particles after the interaction (n = 260, 126, and 318 for anthophyllite, grunerite, and amosite, respectively), the L/w ratio is slightly higher in this range for anthophyllite and grunerite and lower for amosite (Tab. S1 and the complete dataset provided in a separate file).

Starting material (recalculated)

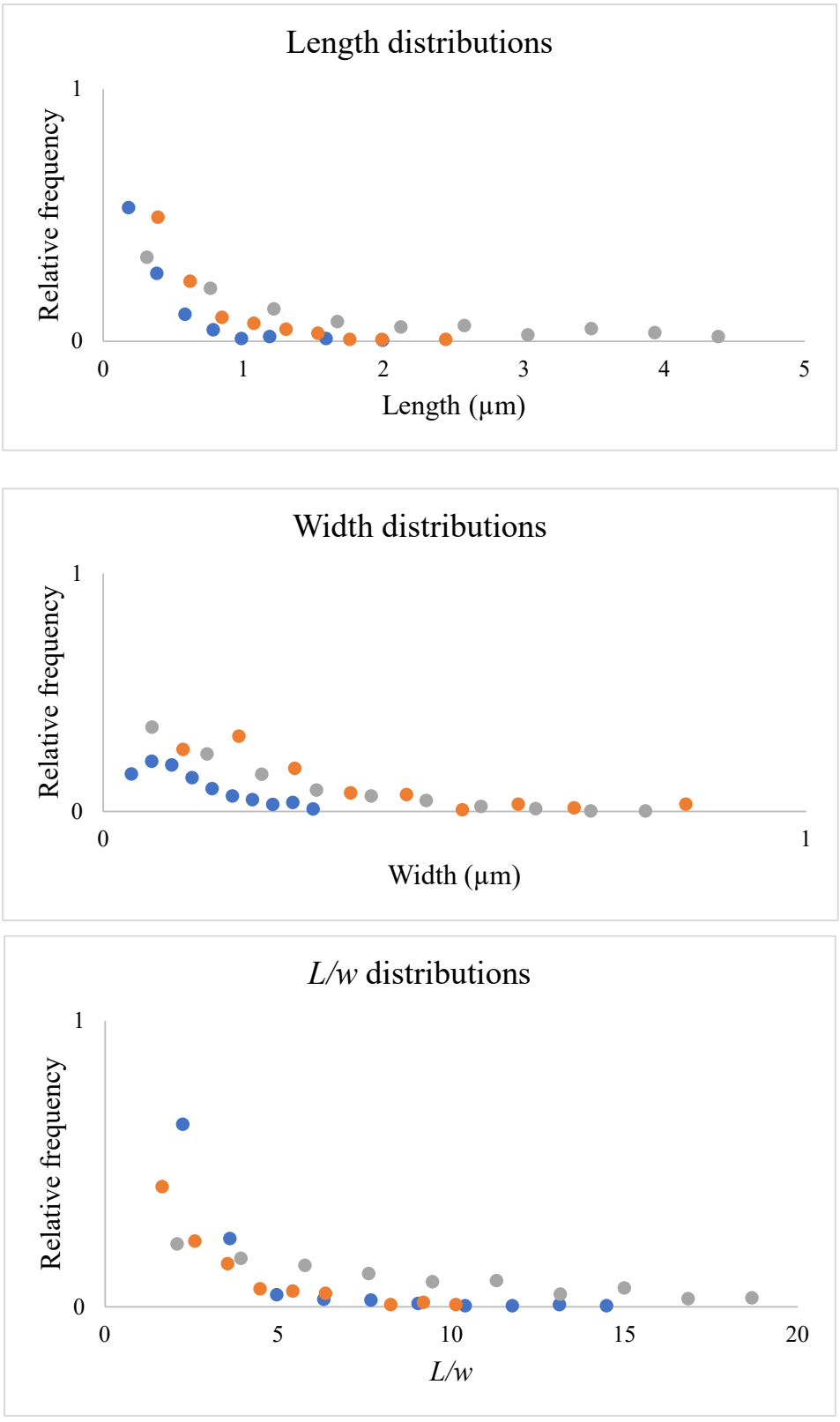

Fig. S1 Dimensional distributions of the particles in the *starting material* considering the range determined by the maximum and minimum dimensions of the retrieved particles (after the interaction). Anthophyllite is in blue, grunerite is in orange, and amosite is in gray.

Tab. S1 Dimensional parameters and aspect ratios of particle populations *before* interaction with the AECs. Here, we considered the range determined by the maximum and minimum dimensions of the retrieved particles (after the interaction).

	Anthophyllite (*n* = 260)				**Grunerite (*n* = 126)**				**Amosite (*n* = 318)**			
	L **(µm)**	***W*** **(µm)**	***L/w***	**% of particles with *L/w* ≥3:1**	***L*** **(µm)**	***w*** **(µm)**	***L/w***	**% of particles with *L/w* ≥3:1**	***L*** **(µm)**	***W*** **(µm)**	***L/w***	**% of particles with *L/w* ≥3:1**
Mean	0.34	0.12	3.08	33.08	0.64	0.26	2.96	36.51	1.28	0.19	7.30	78.30
σ_{n-1}	0.28	0.06	1.93		0.40	0.17	1.80		1.13	0.14	4.70	
Max.	1.99	0.30	14.16		2.46	0.86	10.54		4.51	0.80	18.60	
Min.	0.08	0.03	1.56		0.27	0.07	1.18		0.08	0.03	1.15	

Localization of mineral particles within the cells

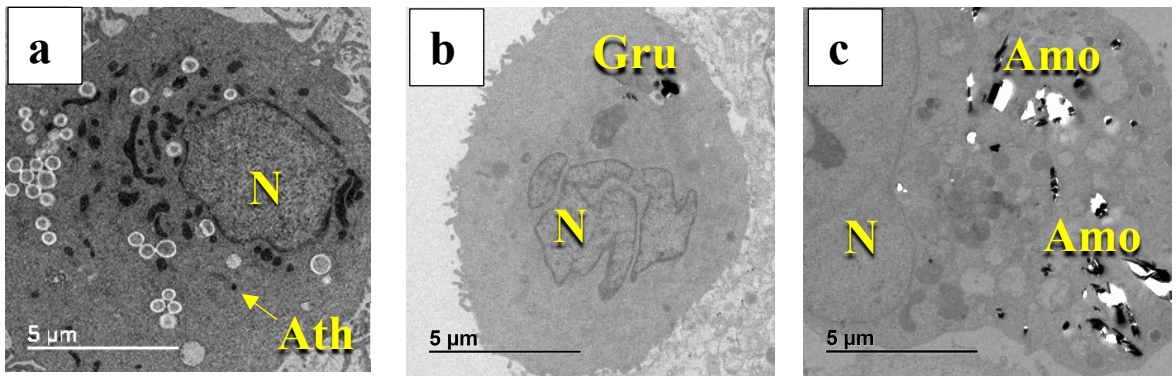

Fig. S2 Low-magnification TEM images of AECs containing **(a)** anthophyllite (**Ath**); (**b)** grunerite (**Gru**); and (**c)** amosite (**Amo**) after 48 h of exposure. **N**: cell nucleus.

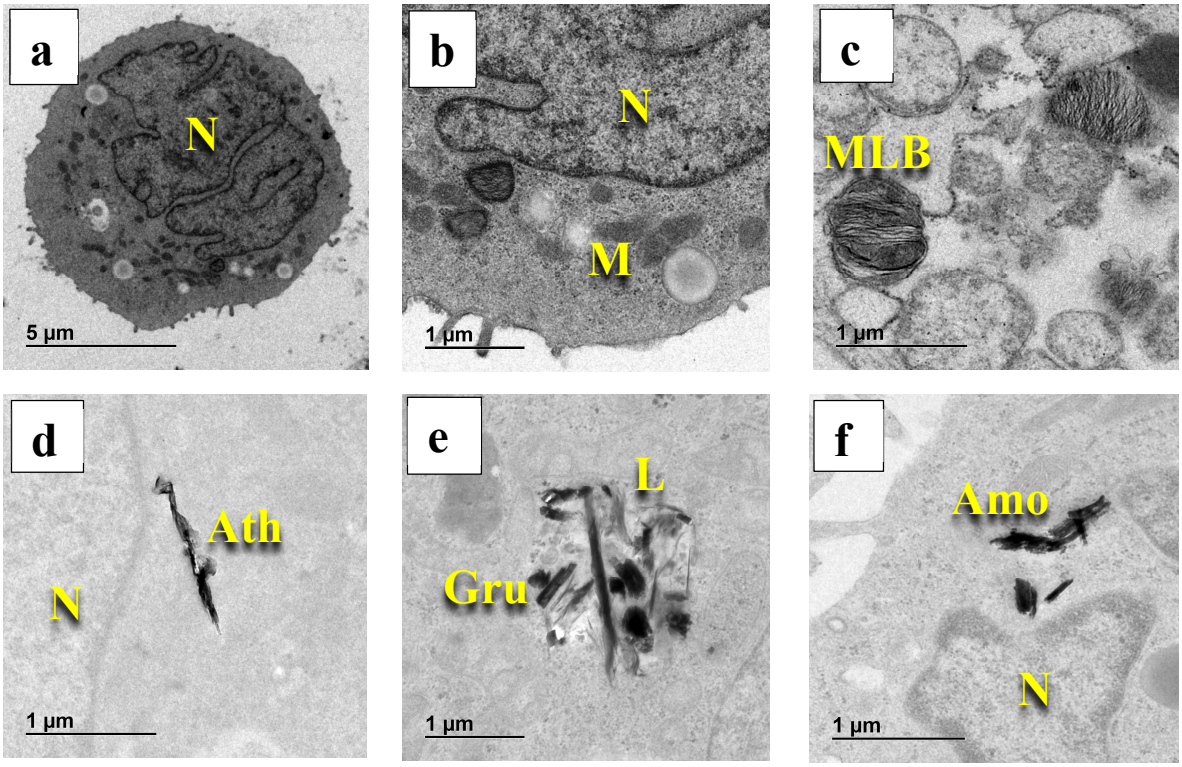

Fig. S3 Low-magnification TEM images of AECs: (**a)** and (**b)** control cells with irregularly shaped nuclei (**N**) and many mitochondria (**M**); (**c)** multilamellar bodies (**MLBs**) in control cells; (**d)** anthophyllite particle (**Ath**) in proximity to the nuclear membrane; (**e)** several grunerite particles (**Gru**) contained in a lysosome (**L**); **(f)** amosite particle (**Amo**) near the nucleus.

Viability and ROS production of cells

Cell viability

We seeded A549 cells on microtiter plates and treated them with serial dilutions of the three different mineral suspensions. The highest concentration used was 100 µg/mL. Treatments with different asbestos concentrations for 48 h did not show a clear dose-dependent effect on viability (Fig. A4), and, in general, we observed culture expansion. At the end of the 48 h exposure, the control cells reached confluence.

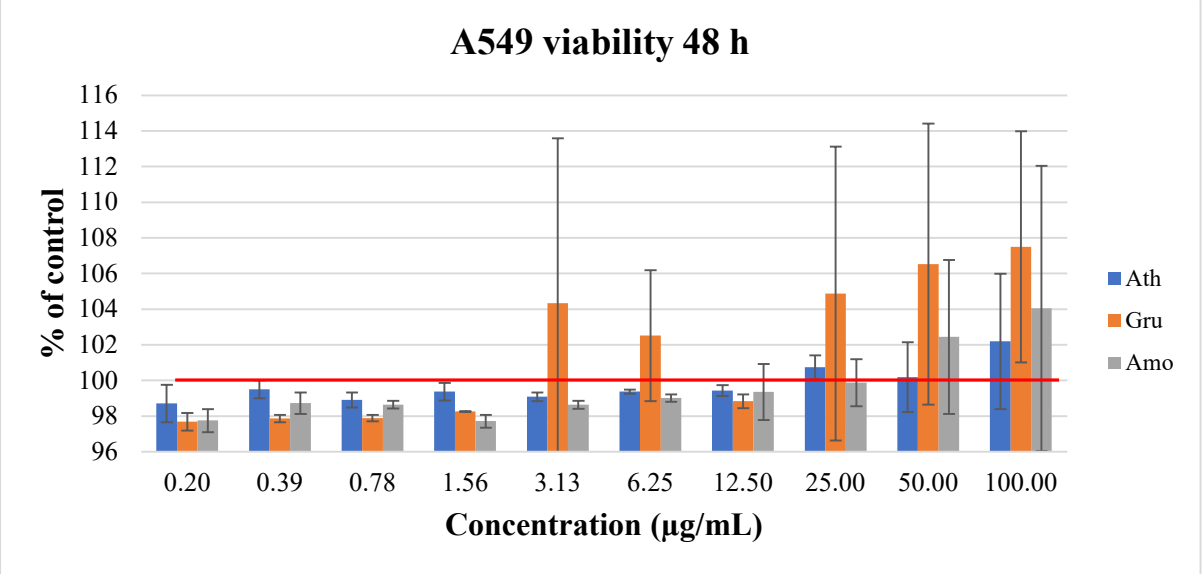

Fig. S4 Cell viability (% of control) for different concentrations of amphiboles. The red line represents the untreated (negative) control (100%).

Measurement of intracellular ROS and H_2O_2

ROS (Fig. A5) and H_2O_2 (Fig. S6) detection was performed on A549 cells and evaluated for a concentration of 50 µg/mL of each mineral 8, 24, and 48 hours after treatment. As a positive control, we used 20 ng/mL of TNFα.

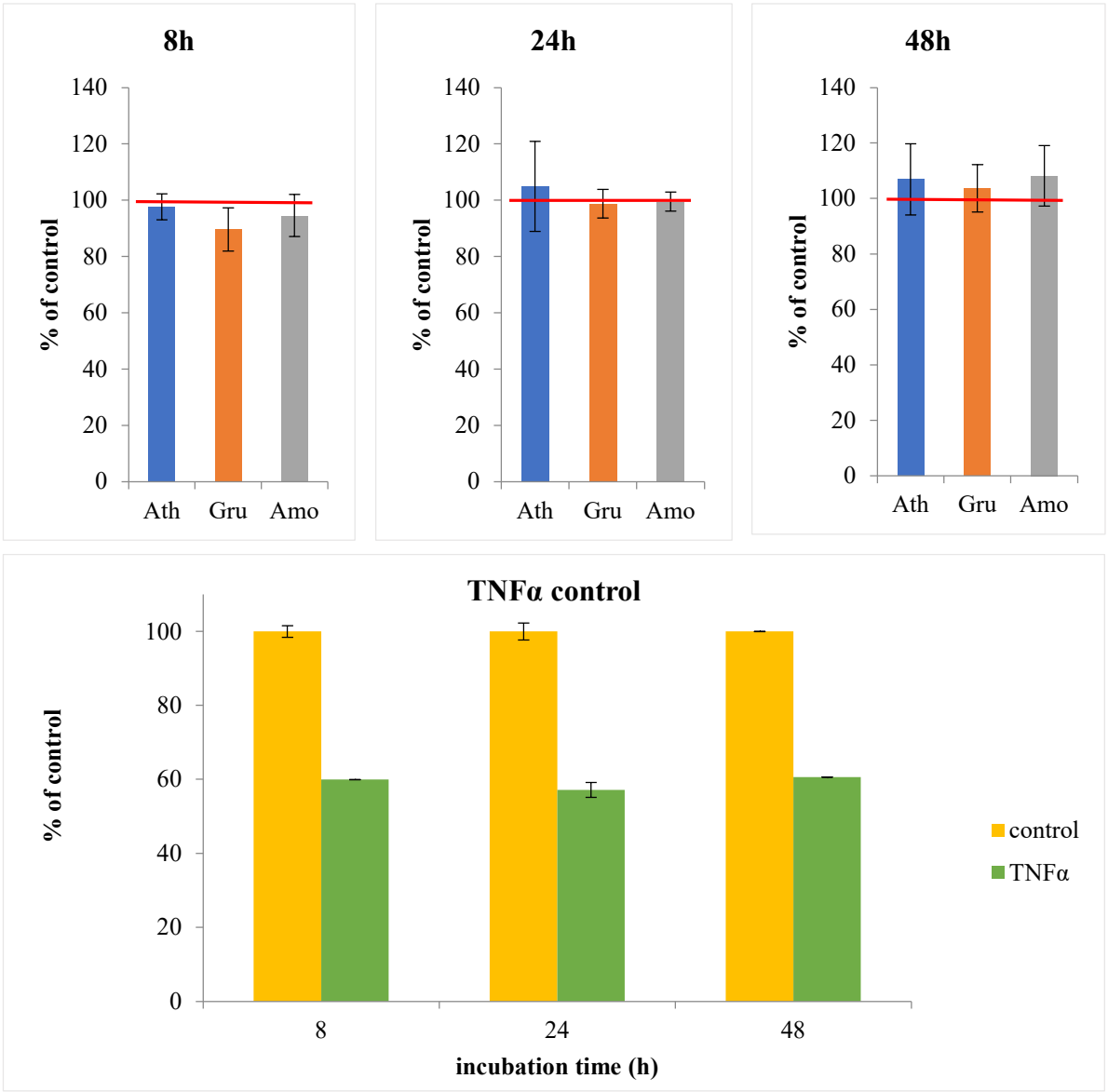

Fig. S5 ROS (Sigma MAK142) measurements conducted using a concentration of 50 µg/mL of each mineral and the related TNF (positive) control. The results are expressed as % of the negative control. The red line/bar represents the untreated (negative) control (100%).

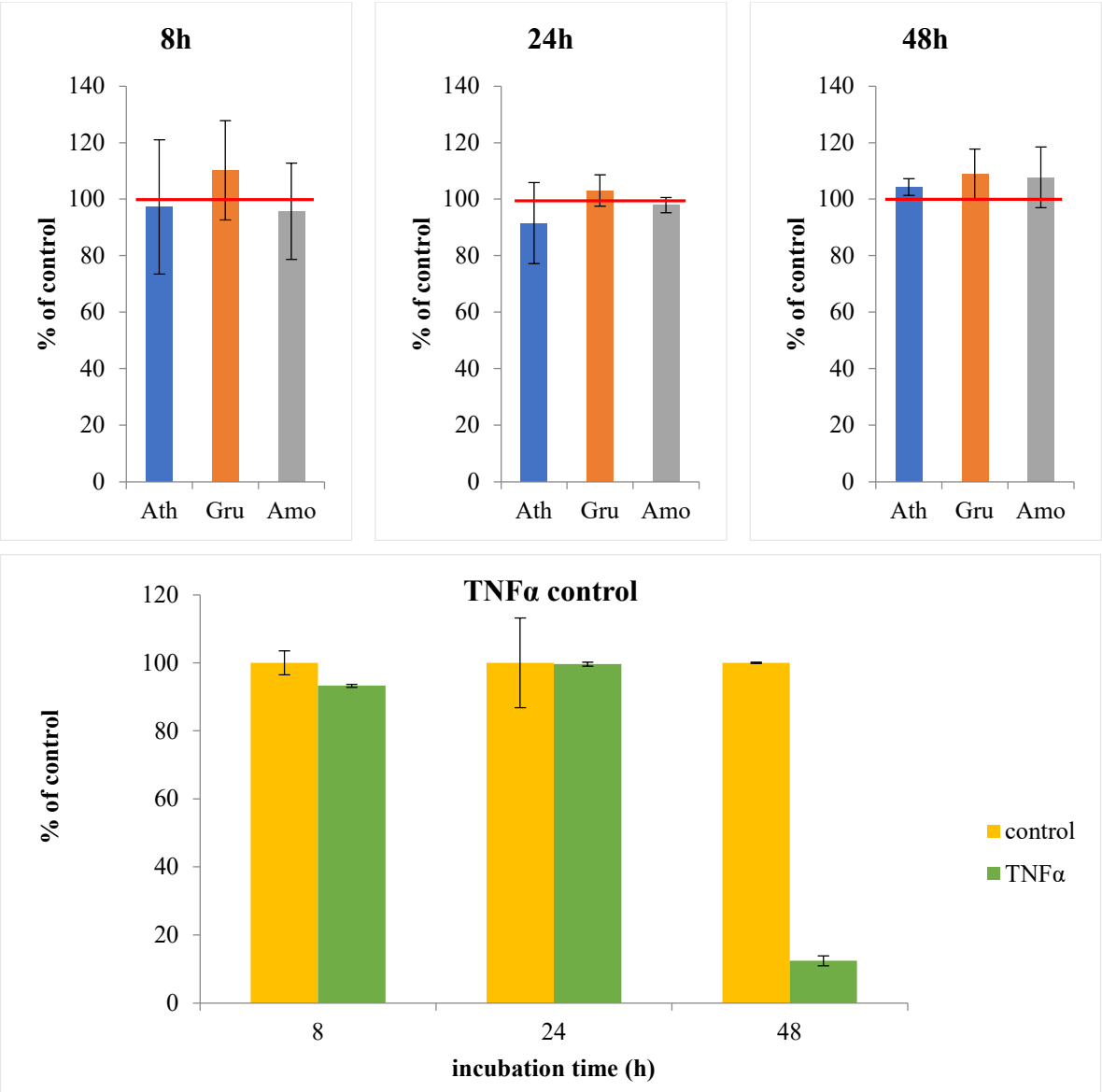

Fig. S6 H_2O_2 (Sigma MAK 165) test conducted using a concentration of 50 µg/mL of each mineral and the related TNF (positive) control. The results are expressed as % of the negative control. The red line/bar represents the untreated (negative) control (100%).

The non-significant effects of the amphibole particles, determined via the ROS (including H_2O_2) and viability assays, may be partly due to the short exposure time and the natural ability of cells to counteract redox reactions, as well as to the observed particle "entombment" by the Fe^{3+}-rich, poorly reactive amorphous layer around the amphibole grains.